Characterization of OAM Antenna Operating in a Multiplexing State

Characterization of OAM Antenna Operating in a Multiplexing State

Zuxian He
State Key Laboratory on Integrated Optoelectronics
College of Electronic Science and Engineering
International Center of Future Science, Jilin University
Changchun, China
hezx19@mails.jlu.edu.cn

Vladimir R. Tuz
State Key Laboratory on Integrated Optoelectronics
College of Electronic Science and Engineering
International Center of Future Science, Jilin University
Changchun, China
School of Radiophysics, Biomedical Electronics and Computer Systems, V. N. Karazin Kharkiv National University
Kharkiv, Ukraine
tvr@jlu.edu.cn

Patrizia Savi
Electronics and Telecommunications Department (DET)
Politecnico di Torino
Torino, Italy
patrizia.savi@polito.it

Dmytro Vavriv
Department of Microwave Electronics
Institute of Radio Astronomy
National Academy of Sciences of Ukraine
Kharkiv, Ukraine
vavriv@rian.kharkov.ua

Volodymyr Fesenko
Department of Microwave Electronics,
Institute of Radio Astronomy
National Academy of Sciences of Ukraine
Kharkiv, Ukraine
volodymyr.i.fesenko@gmail.com

***Abstract*—Orbital angular momentum (OAM), which characterizes the helical phase pattern of optical beams, has recently attracted enormous interest due to its potential applications in different practice areas. Here we propose an antenna design for generating multiple beams carrying OAM with different topological states at the same frequency. The numerical full-wave simulation is performed for an actual size OAM generator using the ANSYS HFSS electromagnetic solver, and an antenna prototype operating in the microwave band is fabricated and tested. Obtained results prove that the proposed antenna can be used as a compact and low-cost generator of multiple beams with different OAM states.**

***Index Terms*—Microwave; Antenna design; Orbital angular momentum**

I. Introduction

Orbital angular momentum, which characterizes the helical phase pattern of optical beams, has recently attracted enormous interest for different applications, e.g., high-resolution imaging, astronomy, quantum optics, and biomedical engineering [1]–[4]. Moreover, there is a significant interest in the use of OAM beams for wireless and optical communications [5], [6].

In the field of wireless and optical communications, increasing the transmission capacity of communication channels is one of the priority tasks that arise in the development of new systems. In such systems wavelength-division multiplexing (WDM), polarization-division multiplexing (PDM), and space-division multiplexing (SDM) are the most common techniques used to increase the transmission capacity [7]. A special case of the SDM is the mode-division multiplexing (MDM), in which a set of mutually orthogonal spatially overlapping and co-propagated modes can carry independent data channels at the same carrying frequency [8], [9]. Several different types of orthogonal modal basis sets can be considered as potential candidates in this case. One of them is a set of OAM modes. Compared to other MDM implementation methods, the combined OAM-MDM technique has some advantages due to its circular mode symmetry, making it suitable for many communication technologies. The OAM-MDM is wavelength and polarization independent, so it can be additionally combined with either WDM or PDM technique to increase the capacity in both wireless and optical communication systems.

In wireless communication systems, microstrip resonator antennas (patch antennas) are commonly used. The convenience of these antennas comes from their easy fabrication, low cost, compact size, and low radiation loss. Compared with the resonators having simpler geometries, antennas based on microstrip ring-shaped resonators are more suitable for the complex system. Circular ring patches in combination with other elements can form compact multi-band antenna systems with a fixed aperture size. This can be implemented by arranging single or several high-frequency radiating elements within the aperture of a ring-shaped antenna. Several designs of such combined emitters have been proposed for the use in the dual-band operations [10] and dual-OAM modes generation [11].

In this Report, we present characteristics of a compact and low-cost generator of multiple beams with different OAM states which can operate at different frequencies. Proposed antenna is composed of a set of microstrip circular ring resonators (CRRs) placed on the top of a dielectric substrate with a ground plane on the bottom side. At the first stage, we fix the resonant frequency f_c and determine analytically all geometric parameters of the antenna. An analytical solution for the radiated field of a single CRR antenna was derived involving the cavity model and the magnetic current approach [12]. Then, in the second stage, we numerically and experimentally characterize the antenna at the resonant frequency

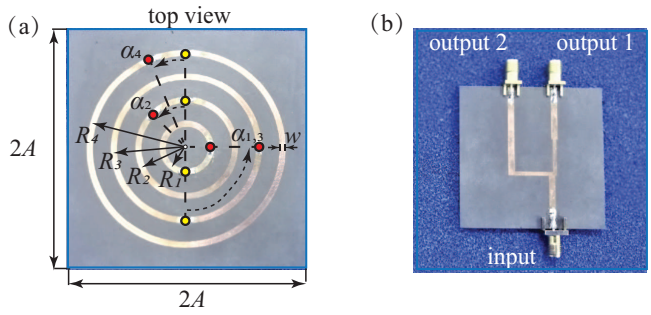

Fig. 1. (a) Photos of the antenna prototype and (b) power divider providing $\pi/2$ phase shift between its output ports. The coaxial probes (CPs) positions are marked by colored circles in the panel (a). The geometrical parameters of the antenna are: $A = 43$ mm, $R_1 = 8.71$ mm, $R_2 = 17.42$ mm, $R_3 = 26.13$ mm, $R_4 = 34.84$ mm, and $w = 2.16$ mm. The substrate is made of Rogers RT/duroid 5880 plate with relative permittivity $\varepsilon_r = 2.2$ and thickness $h = 0.787$ mm.

chosen. For all our subsequent numerical calculations we use the commercial ANSYS High Frequency Structure Simulator (HFSS).

II. Prototype and Experimental Setup

A photo of the designed OAM-MDM antenna prototype is presented in Fig. 1(a). The antenna is composed of four concentric microstrip ring resonators which have the same width $w = 2.16$ mm and different mean radii $R_m = (a_m + b_m)/2$, where a_m and b_m are radii of the inner and outer edges of the corresponding CRR, respectively. The chosen width w of the CRRs provides the characteristic impedance $Z_w = 50$ Ohm of the microstrip line.

For the antenna under consideration, the ratio between the width w of each microstrip ring to its mean radius R_m lies within the range $0.055 \leq w/R_m \leq 0.24$. For such narrow rings, equation that determines the resonant frequencies of the TM_{mn} modes are:

$$k_{mn}R_m = m, \quad \text{when} \quad w/R_m \lesssim 0.25, \tag{1}$$

and the mean radii of the ring-shaped resonators at the corresponding carrier frequency f_c can be determined from Eq. (1) as follows:

$$R_m = cm/(2\pi f_c\sqrt{\varepsilon_{\text{eff}}}), \tag{2}$$

where ε_{eff} is effective permittivity of the substrate which can be defined from the empirical relation [12], [13].

Values of the mean radii R_m obtained using equation (2) are collected in the caption to Fig. 1. From here one can conclude that parameters of our antenna satisfy the following conditions: $h \ll 2R_m$ and $w < 0.5c/f_c$, so the field in the individual CRR can be considered in the single mode approximation, when the resonator operates on a particular TM_{m1} mode.

To feed each of the CRRs of the antenna, a schema with two coaxial probes (CPs) is used. To feed the signal to CRRs, holes with a diameter of 1 mm are drilled in the substrate at the position of the coaxial probes. The CPs are supplied with the same amplitude and relative phase shift of $\pi/2$ to excite two mutually orthogonal TM_{m1} modes on each rings [14]. The correct angular distance α_m between two CPs located on the ring can be determined from the next condition: one

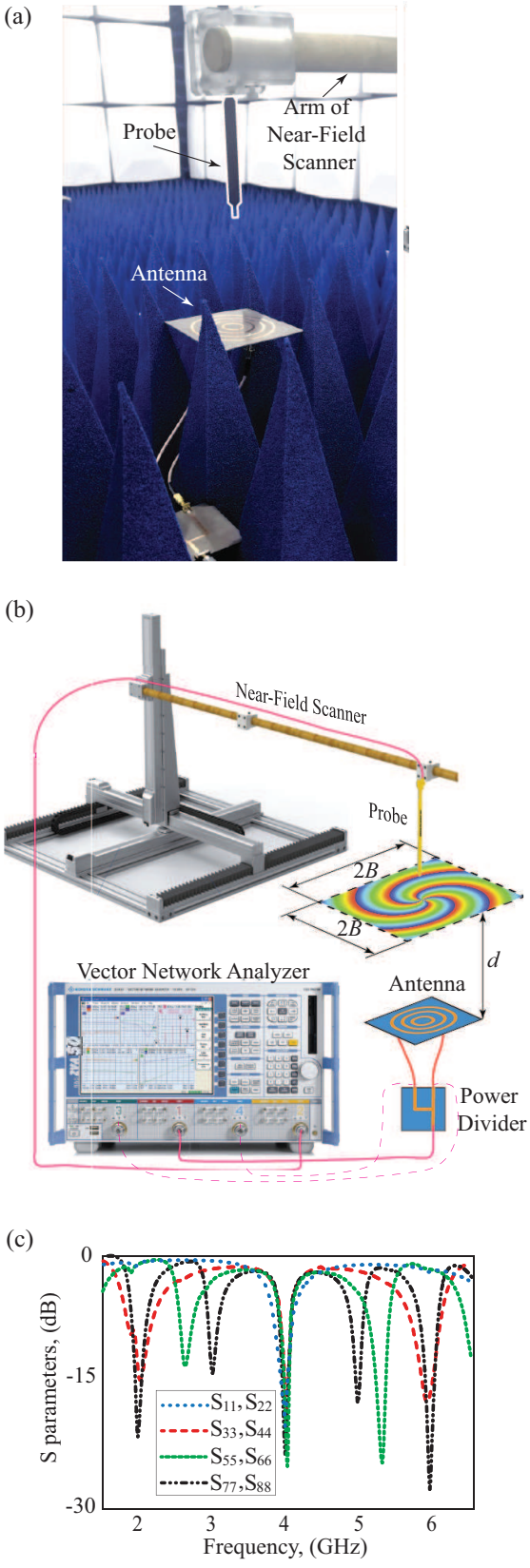

Fig. 2. (a) Photo, (b) schematic view of the experimental setup, and (c) actual S-parameters of the antenna.

coaxial probe is always situated in the null field region of the other probe. This condition yields the following angles: $\alpha_1 = \alpha_3 = \pi/2$, $\alpha_2 = \pi/4$, $\alpha_4 = \pi/8$. To obtain the equal magnitude and $\pi/2$ phase difference of two CPs, a 3-

dB Wilkinson power divider was designed. It is presented in Fig. 1(b). In this device, the $\pi/2$ phase difference is realized by a quarter-wavelength differential line length between two arms of the output ports [15], [16]. For a simultaneous supply of several ports in the multiplexing regime, a standard power divider is used.

For the m-th CRR, this feed schema allows us to generate OAM mode with topological charge numbers $|l| = m$ at the chosen operating frequency. Such OAM modes are mutually orthogonal. They can be multiplexed together and transmitted along the same spatial axis and then demultiplexed with a low crosstalk [6]. Thus, by simultaneously exciting several CRRs, the given antenna can generate multiple OAM modes with different states l at the same carrier frequency f_c providing the conditions for operating in the OAM-MDM regime [17]. According to the experimental means at our disposal, we choose to characterize the antenna which simultaneously generates the multiple topological states $l = 2, -3, 4$ at the frequency $f_c = 4$ GHz, and study its performance.

The technical details of our experimental setup are shown in Fig. 2. The Rohde & Schwarz Vector Network Analyzer (VNA) ZVA50 generates the primary signal and connects the power dividers with the 50 Ohm coaxial cable. The signals from the output port of the power divider are fed to the corresponding coaxial probes. These probes are inner pins of SMA connectors that are soldered to the hole of the ring metallization. The designed antenna is placed in the absorbing material in the x-y plane. The LINBOU near-field scanning platform [18] is used to measure the magnitude and phase distribution of the z-component of the electric field (additional details on the experimental method and measurement setup can be found in Ref. [19]).

The near field data of the antenna are collected with the use of the scanning subwavelength electric probe (see Fig. 2(b)). The probe is positioned normally to the surface of the antenna. The distance d between the antenna and the scanning plane is 75 mm. The probe moves in the x-y plane over the scanning area $2B \times 2B$ mm, where $B = 200$ mm. The step width of the scanning area is 10 mm. Additionally, the signals from the output ports of the power divider are fed into auxiliary ports (Port 3 and Port 4) of the VNA to validate the equality of the amplitude and relative phase difference. Actual S-parameters of the antenna are collected in Fig. 2(c). To avoid unwanted reflections, all measurements were performed in an anechoic chamber.

III. Results and Discussion

Since in our experimental setup we have the ability to measure both the phase and amplitude of the z-component of the electric field, we perform our classification of the OAM modes, assuming that the azimuthal mode index m is equal to the absolute value of the topological charge number $|l|$ of the corresponding OAM state. Thereby, from the TM_{m1} mode of the ring-shaped resonator, a beam carrying OAM with topological state $l = \pm m$ appears.

Proposed antenna can produce OAM waves with the left-handed $l = +m$ (wave with the positive helicity) and right-handed $l = -m$ (wave with the negative helicity) spiral structure. In particular, a beam carrying OAM with topological stage $l = +m$ appears when the signal passing through the first coaxial probe (yellow circles in Fig. 1) is behind the signal passing through the second probe (red circles in Fig. 1)) at $\pi/2$.

In the following content, we analyze the characteristics of the OAM antenna operating in a multiplexing state. The analytical, simulated, and measured distributions of the instantaneous phase and amplitude of the z-component of the electric field for the radiated OAM waves with topological charge numbers $l = 2, -3, 4$ are shown in Fig. 3. One can conclude that there is a reasonable agreement between analytical, simulated and experimental data. It can also be seen that when several resonators are simultaneously excited, the helical structure of the released wave is preserved which can be used to implement a multiplex state. The far-field radiation pattern for such a multiplex state is presented in Fig. 4(a).

In the cross-section, the intensity of the center of the OAM beam is zero, and there is a "dark area" near it, which is a distinct feature of the OAM waves [20]. In the experimental data, one can notice some unbalance in the electric field distributions compared to the theoretically predicted ones. It can be explained by our use of a feeding system with two coaxial probes for each resonator.

To obtain qualitative characteristics of the generated field, the modal analysis can be applied. To ensure the possibility of implementing a multiplex state, we compared the OAM content (mode purity) carried by the experimental fields

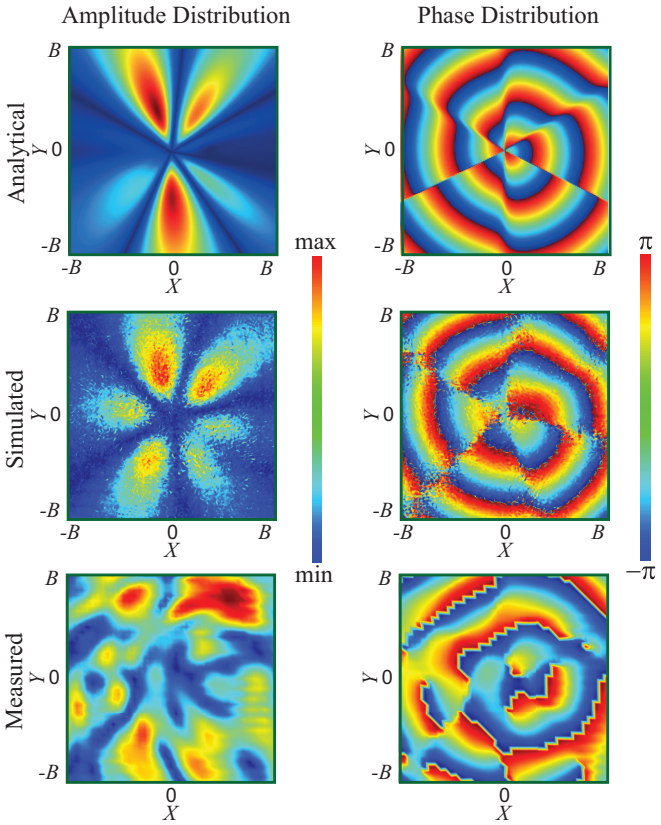

Fig. 3. Analytical, simulated, and measured data for magnitude (left column) and phase (right column) distributions of the z-component of the eclectic field for the multiplex state presented by a superposition of three OAM modes with $l = 2$, $l = -3$, and $l = 4$ for the antenna operating at the fixed frequency $f_c = 4.0$ GHz.

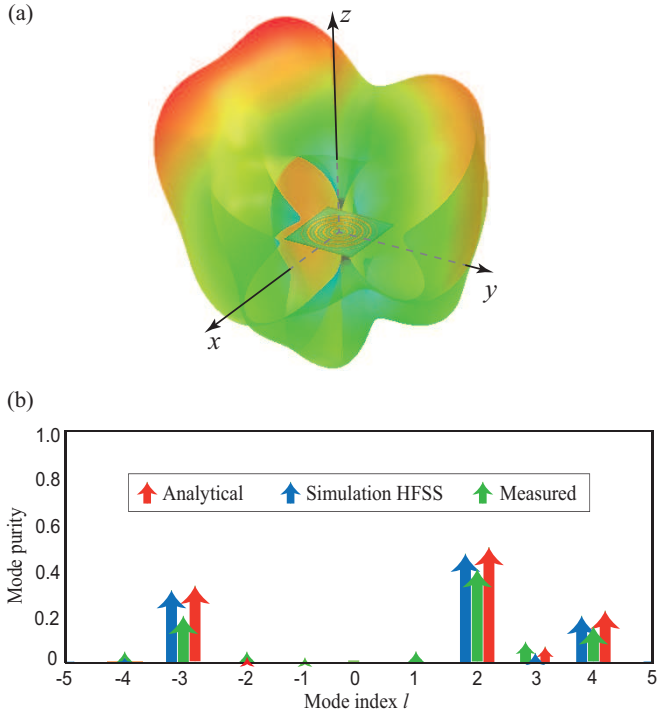

Fig. 4. (a) Far-field radiation pattern for the multiplex state presented by superposition of three OAM modes with $l = 2$, $l = -3$, and $l = 4$. (b) Mode purity for the OAM waves calculated from the data shown in Fig. 3.

with the expected analytical and numerically simulated ones. For this purpose, we applied the spiral spectrum algorithm [21] which performs the projection of the electromagnetic field on spiral harmonics, similarly to the Fourier transform. Corresponding results are collected in Fig. 4(b). There is a correspondence between the obtained results, although there is some crosstalk between the modes of the same topological charge number with different helicity which are derived from the experimental data. This increased crosstalk seems to be related to the near field disturbance that our dipole probe introduces when taking measurements. However, even with this shortcoming, the modes can be uniquely identified in the multiplexing states.

IV. Conclusions

Here, an antenna prototype operating in the microwave band is fabricated and experimentally tested. The characterization of the OAM antenna operating in a multiplexing state is performed. The obtained results show the possibility of using the proposed OAM antenna as a small-size and low-cost generator capable of operating in the OAM-MDM regime. By further modifying the design, an antenna for generating composite OAM beams can be realized.

References

[1] T. Yuan, H. Wang, Y. Qin, Y. Cheng, "Electromagnetic vortex imaging using uniform concentric circular arrays," IEEE Antennas Wirel. Propag. Lett., vol. 14, pp. 1024–1027, 2015.

[2] F. Tamburini, B. Thidé, G. Molina-Terriza, G. Anzolin, "Twisting of light around rotating black holes," Nat. Phys., vol. 7, pp. 195–197, 2011.

[3] A. Vaziri, G. Weihs, A. Zeilinger, "Experimental two-photon, three-dimensional entanglement for quantum communication," Phys. Rev. Lett., vol. 89, pp. 240401, 2002.

[4] Y. Weng, T. Wang, Z. Pan, "Biomedical photoacoustic imaging sensor based on orbital angular momentum multiplexing," *Photonics North.*, IEEE, 2015.

[5] C. Dai, Z. Dong, Y. Zhang, J. Lin, P. Yao, L. Xu, C. Gu, Q. Zhan, "Terabit-scale orbital angular momentum mode division multiplexing in fibers," Science, vol. 340, iss. 6140, pp. 1545–1548, 2013.

[6] Y. Yan, G. Xie, M. Lavery, H. Huang, N. Ahmed, C. Bao, Y. Ren, Y. Cao, L. Li, Z. Zhao, A. F. Molisch, "High-capacity millimetre-wave communications with orbital angular momentum multiplexing," Nat. Commun., vol. 5, pp. 4876, 2014.

[7] D. Tse, P. Viswanath, *Fundamentals of Wireless Communication* (Cambridge University, 2005).

[8] A. E. Willner, H. Huang, Y. Yan, Y. Ren, N. Ahmed, G. Xie, C. Bao, L. Li, Y. Cao, Z. Zhao, J. Wang, M. P. J. Lavery, M. Tur, S. Ramachandran, A. F. Molisch, N. Ashrafi, S. Ashrafi, "Optical communications using orbital angular momentum beams," Adv. Opt. Photon., vol. 7, pp. 66–106, 2015.

[9] W. Zhang, S. Zheng, X. Hui, R. Dong, X. Jin, H. Chi, X. Zhang, "Mode division multiplexing communication using microwave orbital angular momentum: An experimental study," IEEE Trans. Wirel. Commun., vol. 16, pp. 1308–1318, 2017.

[10] J. W. Mink, "Circular ring microstrip antenna elements," *1980 Antennas and Propagation Society International Symposium*, 1980, pp. 605–608.

[11] L. Gui, M. R. Akram, D. Liu, C. Zhou, Z. Zhang, Q. Li, "Circular slot antenna systems for OAM waves generation," IEEE Antennas Wirel. Propag. Lett., vol. 16, pp. 1443–1446, 2017.

[12] R. Garg, P. Bhartia, I. J. Bahl, A. Ittipiboon, *Microstrip Antenna Design Handbook* (Artech house, Boston, 2001).

[13] V. I. Fesenko, G. V. Tkachenko, "Modeling of 1-D photonic bandgap microstrip structures," *2007 International Workshop on Optoelectronic Physics and Technology*, IEEE, 2007.

[14] Q. Zhan, "Cylindrical vector beams: from mathematical concepts to applications," Adv. Opt. Photonics, vol. 1, pp. 1–57, 2009.

[15] S. Wang, Q. Zeng, T. A. Denidni, "Double-OAM-mode generation by octagonal microstrip ring antenna," *2020 IEEE International Symposium on Antennas and Propagation and North American Radio Science Meeting*, (Montreal, 2020), pp. 191–192.

[16] M. Steer, *Fundamentals of Microwave and RF Design* (NC State University, 2019), 3rd ed.

[17] A. D'Errico, R. D'Amelio, B. Piccirillo, F. Cardano, L. Marrucci, "Measuring the complex orbital angular momentum spectrum and spatial mode decomposition of structured light beams," Optica, vol. 4, pp. 1350–1357, 2017.

[18] www.linbou.com.

[19] A. S. Kupriianov, V. R. Tuz, "Microwave approach to study resonant features of all-dielectric metasurfaces," *2019 Photonics Electromagnetics Research Symposium - Fall (PIERS - Fall)*, (Xiamen, 2019), pp. 866-–870.

[20] L. Allen, M. W. Beersbergen, R. J. C. Spreeuw, J. P. Woerdman, "Orbital angular momentum of light and the transformation of Laguerre-Gaussian laser modes," Phys. Rev. A, vol. 45, pp. 8185—8189, 1992.

[21] L. Torner, J. P. Torres, S. Carrasco, "Digital spiral imaging," Opt. Express, vol. 13, pp. 873-–881, 2005.